

## **Supplementary Information for** Coupled Oscillation and Spinning of Photothermal Particles in Marangoni Optical Traps

Hyunki Kim<sup>a,1</sup>, Subramanian Sundaram<sup>b,c,1</sup>, Ji-Hwan Kang<sup>a,d</sup>, Nabila Tanjeem<sup>a,e</sup>, Todd Emrick<sup>a\*</sup>,  
Ryan C. Hayward<sup>a,e\*</sup>

<sup>a</sup> Polymer Science and Engineering, University of Massachusetts, Amherst, MA, USA.

<sup>b</sup> Biological Design Center, Boston University, Boston, MA, USA.

<sup>c</sup> Wyss Institute for Biologically Inspired Engineering, Harvard University, MA, USA.

<sup>d</sup> Chemical Engineering, California State University, Long Beach, CA, USA.

<sup>e</sup> Chemical and Biological Engineering, University of Colorado, Boulder, CO, USA

<sup>1</sup> These authors equally contributed.

\* Corresponding authors: Ryan C. Hayward, Todd Emrick

**Email:** ryan.hayward@colorado.edu, tsemrick@mail.pse.umass.edu

### **This PDF file includes:**

Table S1  
Figures S1 to S15  
Legends for Movies S1 to S5

### **Other supplementary materials for this manuscript include the following:**

Movies S1 to S5

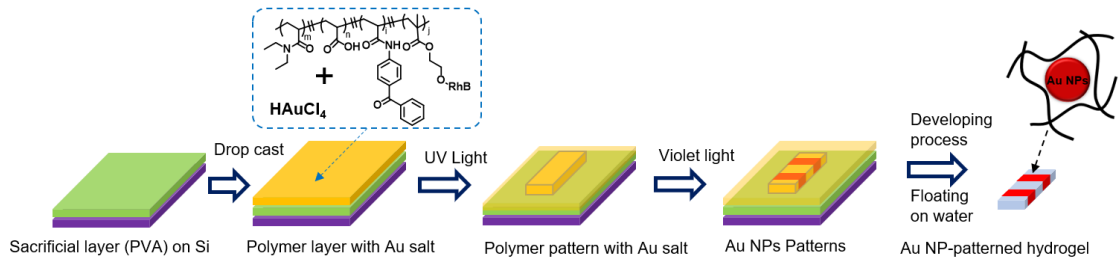
---

Table S1. Model parameters

---

$C_p$	Specific heat capacity (4180 J Kg <sup>-1</sup> K <sup>-1</sup> )
$\mu$	Dynamic viscosity of water (0.890×10 <sup>-3</sup> N s m <sup>-2</sup> )
$\gamma_T$	Temperature coefficient of surface tension, (-0.1379 mN m <sup>-1</sup> K <sup>-1</sup> )
$k_w$	Thermal conductivity of water (0.6 W m <sup>-1</sup> K <sup>-1</sup> )
$k_{th}$	Thermal conductivity of gel (0.6 W m <sup>-1</sup> K <sup>-1</sup> )
$\rho_w$	Density of water (997 Kg m <sup>-3</sup> )
$\rho_m$	Density of gel (997 Kg m <sup>-3</sup> )
$t_d$	Thickness of disk (10 μm)
$a$	Width of disk (300 μm)
$h$	Convection heat transfer coefficient (W m <sup>-2</sup> K <sup>-1</sup> ), from eq. (2)
$R_{th}$	Effective thermal resistance (K W <sup>-1</sup> ), from eq. (3)
$C_{th}$	Effective thermal capacitance (J K <sup>-1</sup> ), from eq. (4)
$\alpha$	Effective optical absorption coefficient of disk
$\Lambda_{drag}$	Effective drag scaling factor
$\Lambda_m$	Effective mass scaling factor
$\Lambda_{th}$	Thermal coupling coefficient

---



**Fig. S1.** Schematic diagram for the fabrication of HNDs by (1) drop-casting on a PVA-coated Si wafer, (2) drop-casting polymer-Au salt solution, (3) patterning hydrogels by UV exposure, (4) patterning Au NPs embedded in the hydrogel using high dose of violet light, (5) development and release of HNDs.

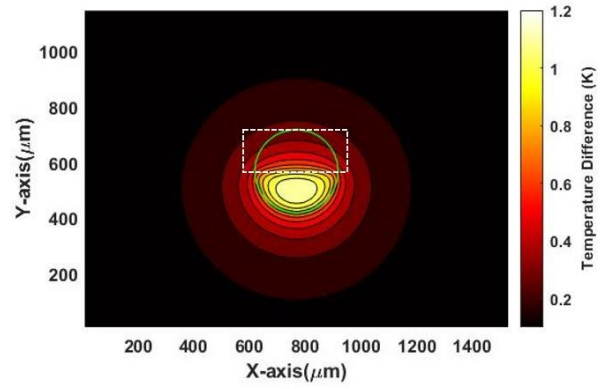


**Fig. S2.** Estimated temperature profile of a circular HND (green circle) located off-center in an optical trap (white dotted line), with light intensity  $3 \text{ W/cm}^2$  using a Green's function approach.

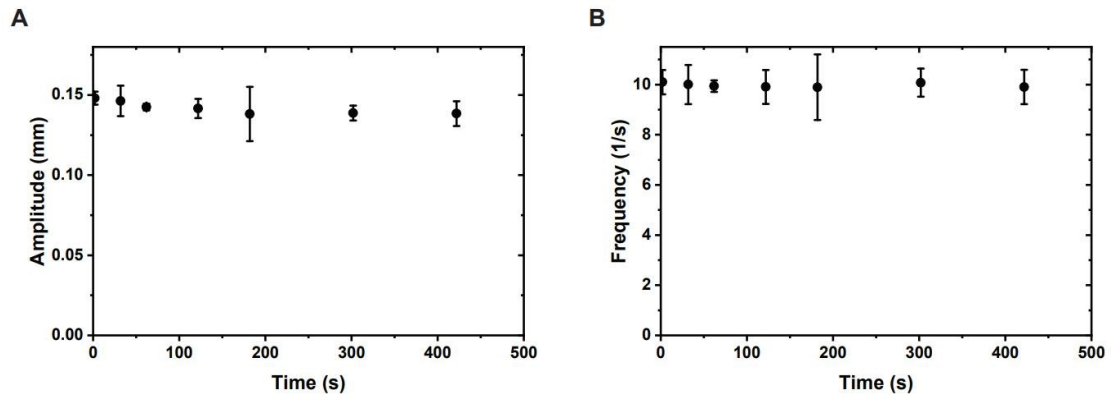


**Fig. S3.** Amplitude (A) and frequency (B) of a single HND oscillator over a period of 400 s (trap height : 140  $\mu\text{m}$ , light intensity: 2.5  $\text{W}/\text{cm}^2$ ).

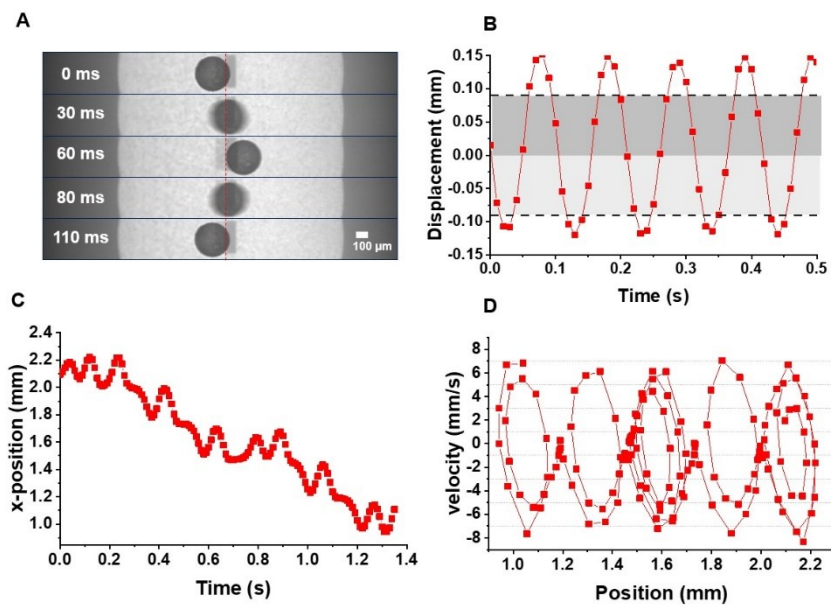


**Fig. S4.** (A) Time-lapse images of oscillating HNDs under asymmetric illumination. (B) Oscillatory motion of HNDs under asymmetric trap patterns, providing off-centered oscillatory motion. (C) Position vs. time plot of trap-hopping HNDs under multiple asymmetric traps as shown in Fig. 1C. (D) Velocity vs. position plot of trap-hopping HNDs from Fig. 1C.

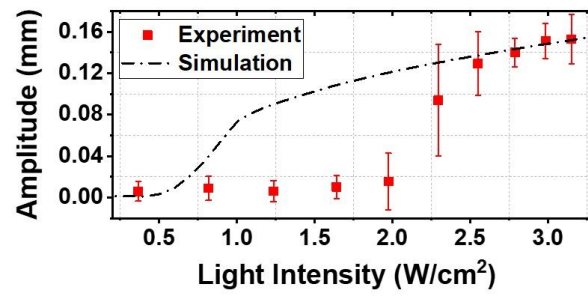


**Fig. S5.** Comparison of HND oscillation amplitudes seen in simulation and experiment under varying light intensity, with a trap height of 140  $\mu\text{m}$ .

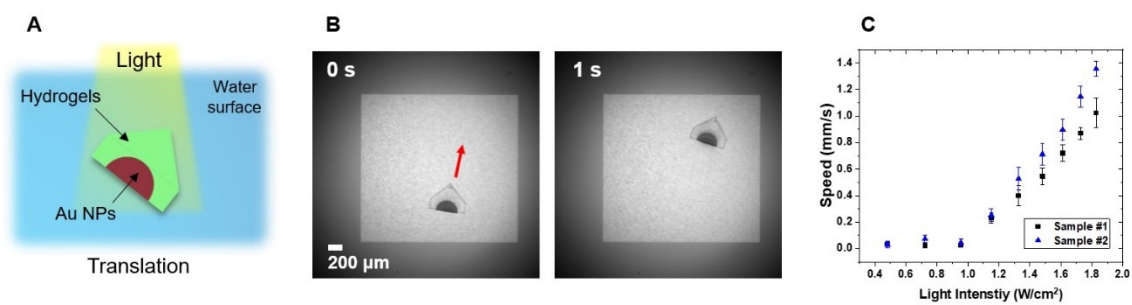


**Fig. S6.** (A) Schematic diagram of HNDs exposed to light, showing unidirectional translation. (B) Time-lapse images of HNDs under light. (C) Speed of the translational motion vs. light intensity of the HNDs with bottom edge length of  $540 \mu\text{m}$ .



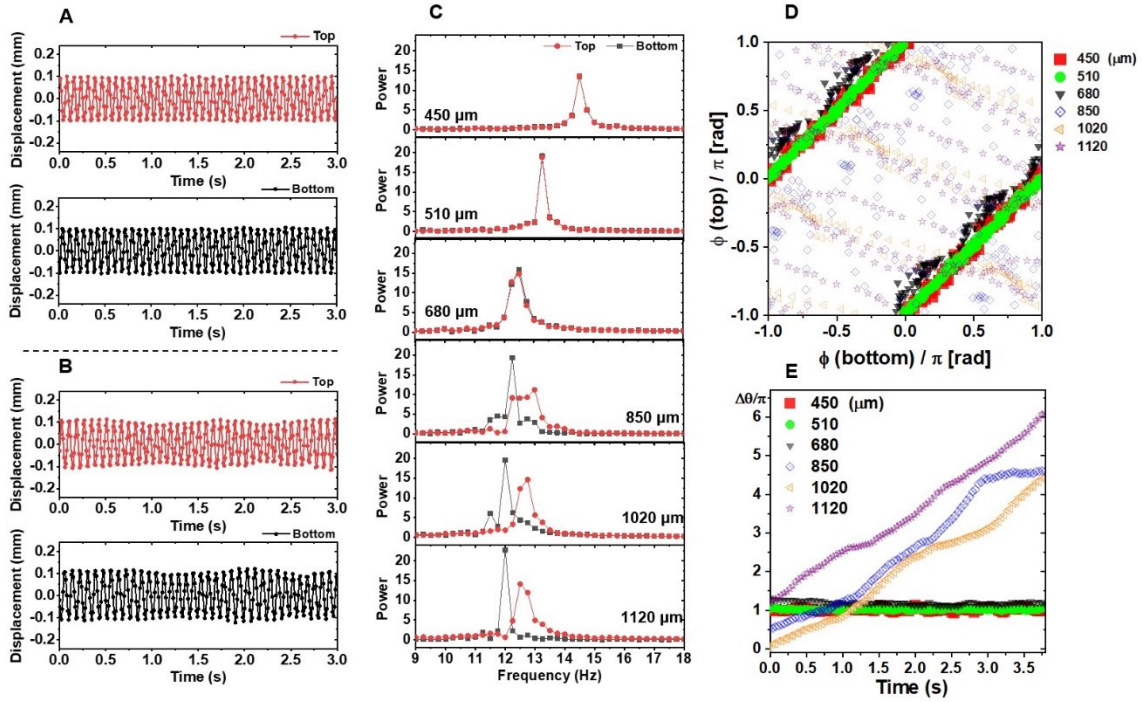


**Fig. S7.** Displacements of 2 coupled HNDs over time with center-to-center trap separation distance of 510 μm (**A**) and 850 μm (**B**). (**C**) Fast-Fourier transforms of the HND oscillations with respect to trap separation distances. (**D**) Phase plots for different trap separation distances. (**E**) Cumulative phase shift between the 2 HNDs over time, for various separation distances.

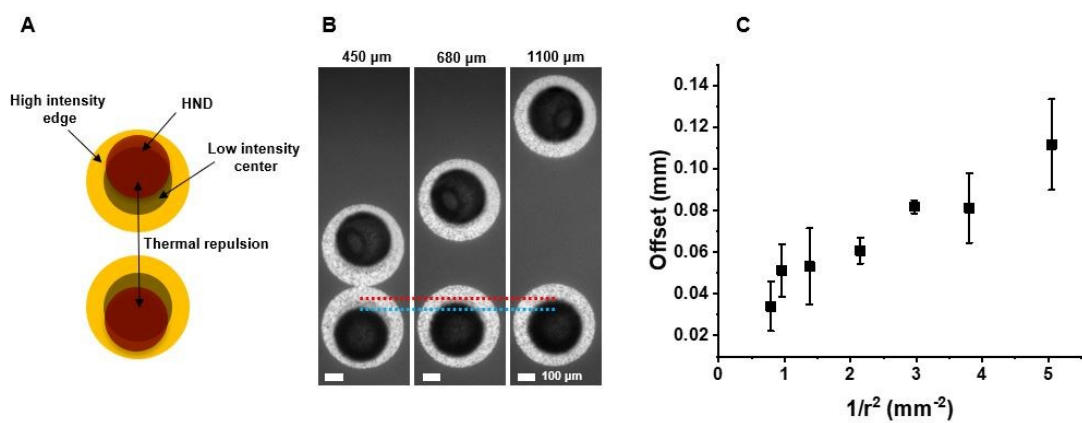


**Fig. S8.** (A) Schematic of the experiment to measure Marangoni repulsion between HNDs in non-oscillatory traps. (B) Images of trapped HNDs with center-to-center trap spacings indicated. (C) Measured offsets of HNDs from the trap centers plotted vs.  $1/r^2$ , where  $r$  is trap separation distance; for the proposed Marangoni repulsion and a trapping force that is linear in offset, the data should follow a straight line.

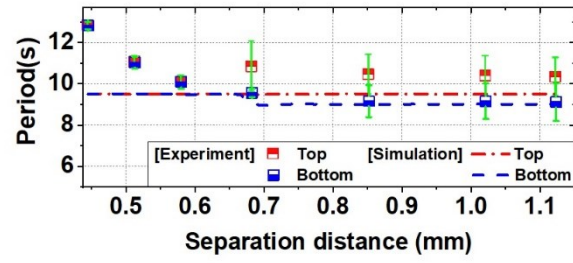


**Fig. S9.** Comparison between simulation and experiment for frequencies of the HNDs under varying separation distances.

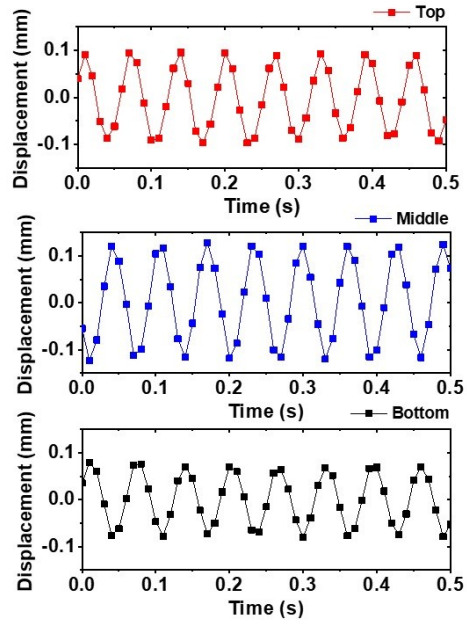


**Fig. S10.** Tracked displacements vs time for the three HNDs under the light pattern described in Fig. 3A.

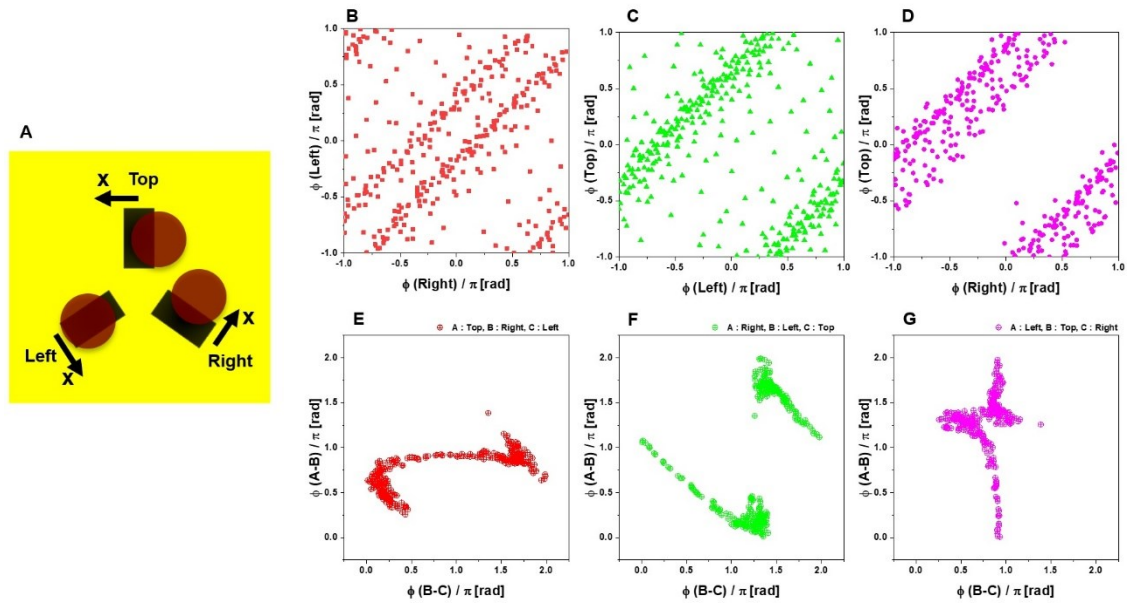


**Fig. S11.** (A) Spatial coordinates for the 3-HND ring oscillator pattern. (B-D) Phase plots for the HND pairs described in Fig. 3C. (E-G) Phase difference maps for HND pairs in the 3-HND ring network.

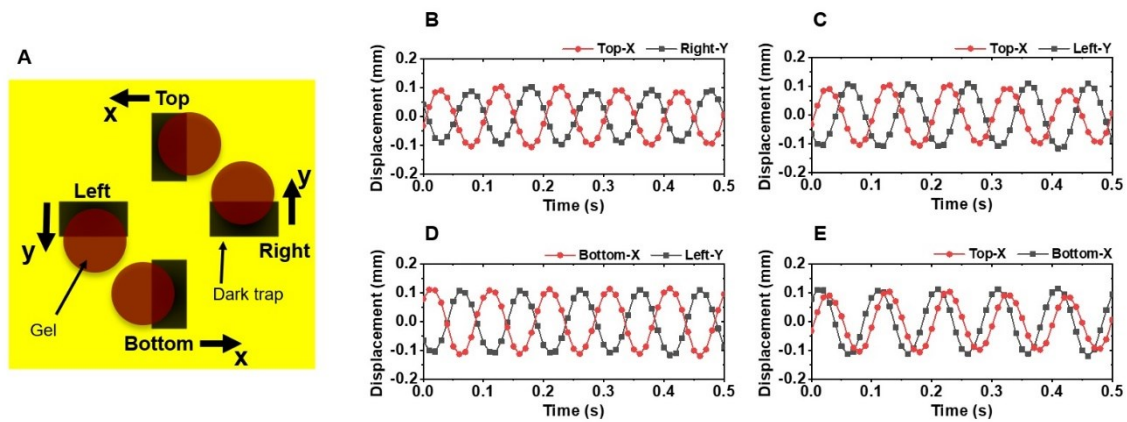


**Fig. S12.** (A) Spatial coordinates for the 4-HND ring pattern. (B-E) Temporal displacements of the four HNDs under the light pattern described in Fig. 3D.

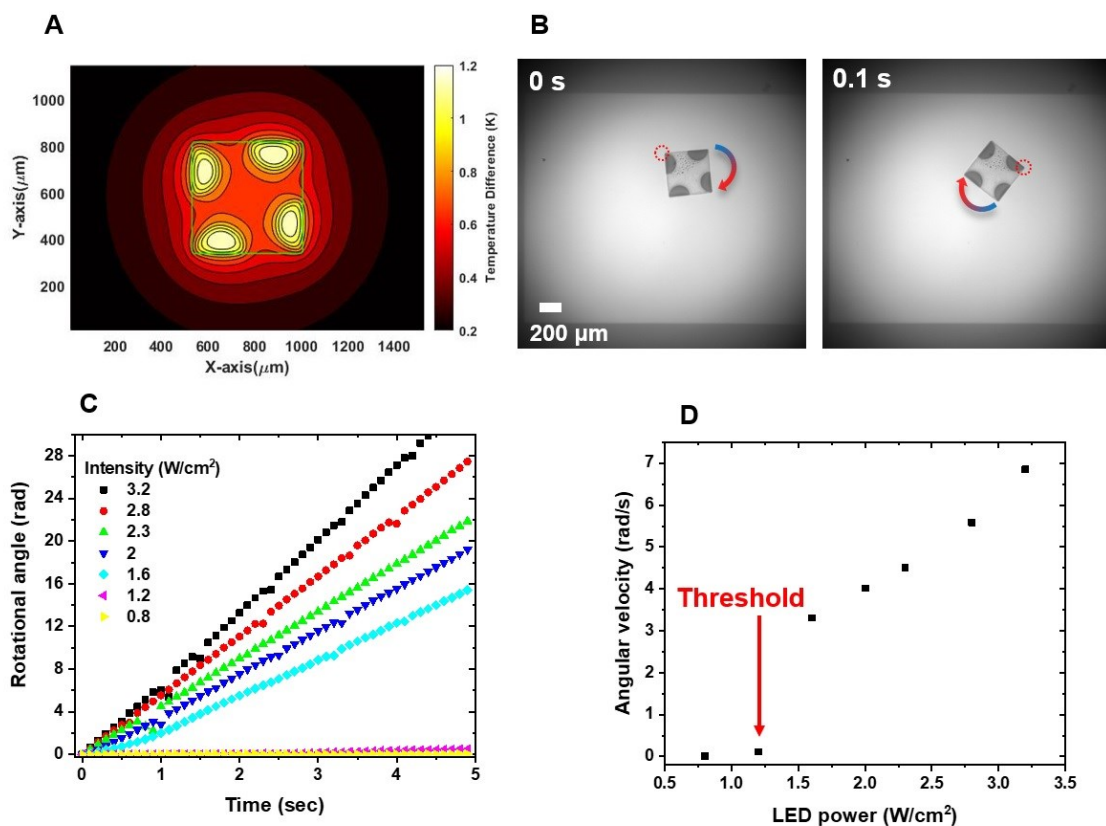


**Fig. S13.** (A) Estimated temperature profile around an HND spinner, subjected to uniform light intensity of  $3 \text{ W}/\text{cm}^2$ , using a Green's function approach. Solid green square line indicates the boundary of the gel. (B) Time-lapse images showing rotational motion under uniform illumination. (C) Variation of the rotational angle over time as a function of light intensity for HND spinners with edge length of  $530 \mu\text{m}$ . (D) Angular velocity vs. light intensity for HND spinners. A threshold intensity to achieve spinning is observed, consistent with observations in the case of HND oscillation (Fig. S5) and propulsion (Fig. S6).

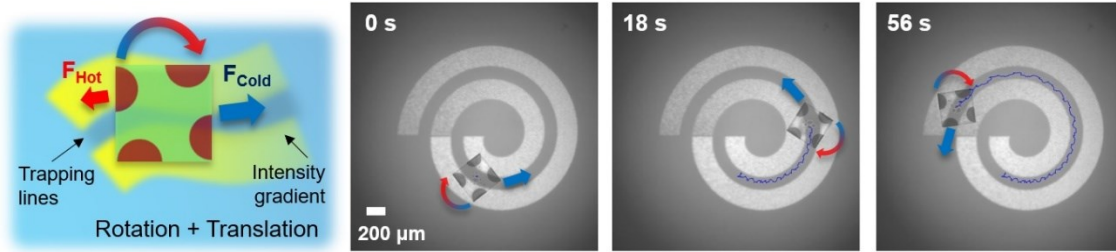


**Fig. S14.** An HND spinner following a path from high to low light intensity.



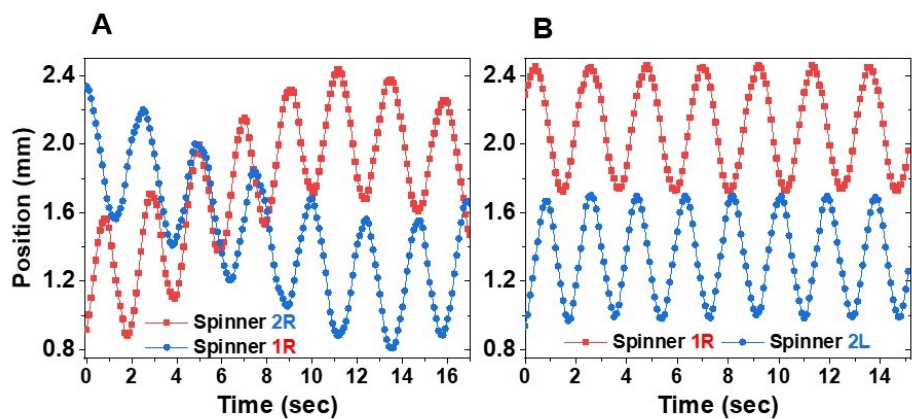


**Fig. S15.** Positions (y-axis) of the corners of square HNDs with respect to time for the two spinners in the Figure. 4G left (A) and right (B).

**Movie S1 (separate file).** Oscillatory motion of single HND under optical traps.

**Movie S2 (separate file).** 1D coupled oscillatory motion of HNDs.

**Movie S3 (separate file).** 2D coupled oscillatory motion of HNDs.

**Movie S4 (separate file).** Spinning and translational motions of gold nanoparticle patterned HNDs.

**Movie S5 (separate file).** Coupling of HND spinners under optical confinement.